DISTILLING REINFORCEMENT LEARNING ALGORITHMS FOR IN-CONTEXT MODEL-BASED PLANNING

Jaehyeon Son[1], **Soochan Lee**[2], **Gunhee Kim**[1]
[1]Seoul National University, [2]LG AI Research
sjh9876@snu.ac.kr, soochan.lee@lgresearch.ai, gunhee@snu.ac.kr

ABSTRACT

Recent studies have demonstrated that Transformers can perform in-context reinforcement learning (RL) by imitating a source RL algorithm. This enables them to adapt to new tasks in a sample-efficient manner without parameter updates. However, since the Transformers are trained to mimic the source algorithm, they also reproduce its suboptimal behaviors. Model-based planning offers a promising solution to this limitation by allowing the agents to simulate potential outcomes before taking action, providing an additional mechanism to deviate from the source algorithm's behavior. Rather than learning a separate dynamics model, we propose Distillation for In-Context Planning (DICP), an in-context model-based RL framework where the Transformer simultaneously learns environment dynamics and improves policy in-context. With experiments across a diverse set of discrete and continuous environments such as Darkroom variants and Meta-World, we show that this method achieves state-of-the-art performance, requiring significantly fewer environmental interactions than the baselines including both in-context model-free counterparts and existing meta-RL methods.

1 INTRODUCTION

Since the advent of Transformers (Vaswani et al., 2017), their flexibility in handling a wide range of tasks has been recognized across numerous fields (Brown et al., 2020; Dosovitskiy et al., 2021; Bubeck et al., 2023). In particular, the in-context learning ability of Transformers (Brown et al., 2020) has garnered significant interest, as it enables the rapid acquisition of knowledge without requiring parameter updates through iterative gradient descent. Consequently, recent studies have explored the application of Transformers' in-context learning ability to the problem of reinforcement learning (RL) (Chen et al., 2021; Schulman et al., 2017; Lee et al., 2022; Reed et al., 2022). Furthermore, this approach has been naturally extended to the meta-RL paradigm, enabling rapid adaptation to novel tasks through in-context learning.

In this context, Laskin et al. (2023) introduce Algorithm Distillation (AD), an in-context RL approach where Transformers sequentially model the entire learning histories of a specific RL algorithm across various tasks. The goal is for the models to replicate the exploration-exploitation behaviors of the source RL algorithm, enabling them to tackle novel tasks in-context. Beyond replication, Laskin et al. (2023) show that this approach can improve the sample efficiency of the source algorithm by bypassing intermediate learning steps or distilling histories from multiple actors. This combination of an off-the-shelf RL algorithm with the in-context learning capability of Transformers demonstrates strong potential in enhancing the adaptability of meta-RL (Lee et al., 2023; Liu & Abbeel, 2023; Huang et al., 2024; Zisman et al., 2024; Sinii et al., 2024).

However, prior in-context RL approaches have a notable limitation: they tend to replicate the suboptimal behaviors of the source algorithm. The source RL algorithm updates its policy gradually through gradient descent, sometimes deliberately preventing abrupt changes (Schulman et al., 2015; 2017). As a result, it may take multiple iterations to fully integrate newly discovered information, leading to repeated suboptimal actions during this process. Without a mechanism to deviate from the source algorithm's behavior, existing in-context RL methods (Laskin et al., 2023; Huang et al., 2024; Sinii et al., 2024) inherit these inefficiencies.

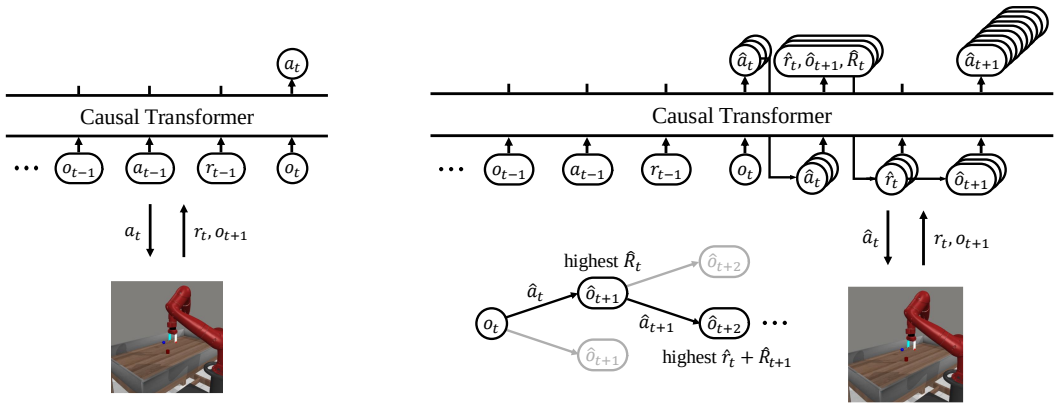

(a) Previous approaches

(b) Distillation for In-Context Planning (Ours)

Figure 1: Comparison between previous approaches (Laskin et al., 2023; Lee et al., 2023; Huang et al., 2024) and our proposed Distillation for In-Context Planning (DICP). Unlike the previous approaches that directly predict actions without modeling dynamics, our approach leverages the in-context learned dynamics model for planning.

To address this limitation, we introduce *Distillation for In-Context Planning (DICP)*, an in-context model-based RL framework where the dynamics model is learned in-context alongside policy improvement. Unlike in-context policy improvement, in-context learning of the dynamics model does not inherit the suboptimal behaviors of the source algorithm, as modeling the environment's dynamics is independent of the inefficiency. By planning with this in-context learned dynamics model, our framework provides the agent with an additional mechanism to overcome the suboptimal behaviors of the source algorithm. Furthermore, simulating potential outcomes before executing actions allows for more deliberate decision-making based on predicted future returns. To the best of our knowledge, ours is the first model-based approach on in-context RL using Transformers to imitate the source algorithm.

To demonstrate the effectiveness of our framework, we conduct experiments in both discrete and continuous environments, including Darkroom variants (Laskin et al., 2023) and Meta-World benchmark suite (Yu et al., 2019). The results indicate that our approach significantly surpasses both in-context model-free counterparts (*e.g.*, AD (Laskin et al., 2023), DPT (Lee et al., 2023), and IDT (Huang et al., 2024)) and existing meta-RL methods (*e.g.*, RL^2 (Duan et al., 2016), MAML (Finn et al., 2017), PEARL (Rakelly et al., 2019), MACAW (Mitchell et al., 2021), FOCAL (Li et al., 2021), BOReL (Dorfman et al., 2021), MoSS (Wang et al., 2023b), and IDAQ (Wang et al., 2023a)). Notably, our method achieves state-of-the-art results on the Meta-World ML1 benchmarks, while requiring significantly fewer environmental interactions compared to the baselines.

2 Related Work

RL as sequence modeling. With the advent of Transformers, which can learn from much larger datasets than what an agent can typically collect online, their adoption to offline RL (Levine et al., 2020) has gained prominence (Chen et al., 2021; Janner et al., 2021; Lee et al., 2022; Reed et al., 2022). Despite these advances, Laskin et al. (2023) point out a key limitation: these approaches struggle to improve their policy in-context through trial and error. The primary reason is that they are designed to imitate the dataset policy, which makes them unsuitable for performing in-context RL on novel tasks. To address this, Laskin et al. (2023) propose Algorithm Distillation (AD), an in-context RL approach where a Transformer is trained to distill learning histories from a source RL algorithm across diverse tasks. Notably, AD becomes effective when the context length of Transformers exceeds the episode horizon. Instead of imitating the source algorithm's actions, Decision-Pretrained Transformer (DPT; Lee et al. (2023)) is designed to predict *optimal* actions. In-context Decision Transformer (IDT; Huang et al. (2024)) implements a hierarchical approach to in-context RL, where the Transformer predicts high-level decisions that guide a sequence of actions, rather than predicting

each action individually. In addition, Sinii et al. (2024) propose an in-context RL approach for variable action spaces, while Zisman et al. (2024) synthesize learning histories by gradually denoising policies instead of directly training a source algorithm.

Meta-RL. Deep meta-RL began with online approaches, where RNNs are employed to learn RL algorithms that generalize across environments (Duan et al., 2016; Wang et al., 2016). In parallel, gradient-based approaches (Finn et al., 2017; Nichol et al., 2018) aim to discover parameter initializations that rapidly adapt to new tasks. Recently, *offline* meta-RL has gained attention, leveraging pre-collected meta-training datasets to address the meta-RL problem (Mitchell et al., 2021; Dorfman et al., 2021; Yuan & Lu, 2022; Wang et al., 2023a;b). Various methods have been explored for this problem, including gradient-based (Mitchell et al., 2021), Bayesian (Dorfman et al., 2021), and contrastive learning approaches (Yuan & Lu, 2022). Furthermore, recent in-context RL approaches (Laskin et al., 2023; Lee et al., 2023; Huang et al., 2024; Sinii et al., 2024), including our own, fall within the category of offline meta-RL.

Model-based meta-RL. In the prior research on model-based meta-RL, Zintgraf et al. (2020; 2021); Dorfman et al. (2021) focus on learning to infer belief states about environment dynamics, while Wang et al. (2023b) aim to infer task representations. Wang et al. (2023a) quantify uncertainty using an ensemble of meta-training dynamics when facing novel meta-test tasks. Nagabandi et al. (2019); Pinon et al. (2022); Rimon et al. (2024) learn to construct dynamics models for planning. Our approach aligns with the latter category but stands out by integrating both the policy and the dynamics model within the same sequence model. This contrasts with prior work that either relies on separate modules for modeling dynamics (Nagabandi et al., 2019; Rimon et al., 2024), or omits a policy network while depending solely on the dynamics model (Pinon et al., 2022). We provide a more comprehensive overview of related works in Appendix D.

3 Problem Formulation

POMDP. We consider a partially observable Markov decision process (POMDP): $\mathcal{M} = (\mathcal{S}, \mathcal{A}, \mathcal{O}, \mathcal{T}, \mathcal{R}, \gamma)$. At each time step t, an agent interacts with the environment by selecting an action $a_t \in \mathcal{A}$ based on the current state $s_t \in \mathcal{S}$. The environment transitions to the next state $s_{t+1} \in \mathcal{S}$ according to the transition model $\mathcal{T}(s_{t+1} \mid s_t, a_t)$, and the agent receives a reward $r_t \in \mathcal{R}$, determined by the reward model $\mathcal{R}(r_t \mid s_t, a_t)$. However, the agent does not directly observe the true state s_t. Instead, it receives partial observation $o_t \in \mathcal{O}$ of the state s_t. The discount factor $\gamma \in [0, 1]$ controls the relative importance of immediate versus future rewards. The tuple $(\mathcal{T}, \mathcal{R})$ is referred to as the *dynamics model* or *world model*. The agent's *history* up to time step t is defined as $h_t = (o_0, a_0, r_0, \dots, o_t, a_t, r_t)$. The objective of RL is to find a policy that maximizes the expected cumulative reward $J = \mathbb{E}_{\pi, \mathcal{M}} \left[\sum_{t=0}^{T} \gamma^t r_t \right]$, where T is the number of interactions. Throughout the paper, we use the terms *environment* and *task* interchangeably to refer to a POMDP.

Meta-RL. We define an *algorithm* $f : \mathcal{H} \times \mathcal{O} \to \Delta(\mathcal{A})$, where $\mathcal{H}$ is the space of histories, and $\Delta(\mathcal{A})$ represents the space of probability distributions over $\mathcal{A}$. The objective of meta-RL is to discover an algorithm f that maximizes the expected cumulative reward J over a distribution of POMDPs $p(\mathcal{M})$. During *meta-training*, the algorithm is optimized on a set of tasks sampled from $p(\mathcal{M})$, while during *meta-test*, it is evaluated on another set of tasks sampled from $p(\mathcal{M})$. For simplicity, we refer to meta-training and meta-test as *training* and *test* when the context is clear.

Following previous works (Laskin et al., 2023; Huang et al., 2024), we focus on scenarios where an offline dataset of learning histories $\mathcal{D} = \{h_T^i = (o_0^i, a_0^i, r_0^i, \dots, o_T^i, a_T^i, r_T^i)\}_{i=1}^n$ is available, generated by a source algorithm f_{source} for a set of meta-training tasks $\{\mathcal{M}_i \sim p(\mathcal{M})\}_{i=1}^n$. The loss function for AD (Laskin et al., 2023) is defined as

$$\mathcal{L}_{\text{AD}}(\theta) = -\sum_{i=1}^{n} \sum_{t=1}^{T} \log f_\theta(a_t^i \mid o_t^i, h_{t-1}^i), \tag{1}$$

where θ represents a sequence model. Similarly, the loss functions for DPT (Lee et al., 2023) and IDT (Huang et al., 2024) are respectively presented in Eq. 3-4 in Appendix.

Algorithm 1 Meta-Training Phase

Required: task distribution $p(\mathcal{M})$, source algorithm f_{source}, sequence model θ
$\mathcal{D} \leftarrow \{\}$
for $i = 1 \dots n$ **do**
  Sample a training task $\mathcal{M}_i \sim p(\mathcal{M})$.
  Train f_{source} on $\mathcal{M}_i$ and collect learning history $h_t^i = (o_0^i, a_0^i, r_0^i, \dots, o_T^i, a_T^i, r_T^i)$.
  $\mathcal{D} \leftarrow \mathcal{D} \cup h_t^i$.
end for
while not converge **do**
  Sample $(o_s, a_s, r_s, \cdots, o_{s+k}, a_{s+k}, r_{s+k})$ from $\mathcal{D}$.
  Optimize θ for Eq. 2 with the sampled trajectory.
end while

Algorithm 2 Meta-Test Phase

Required: task distribution $p(\mathcal{M})$, sequence model θ
for $j = 1 \dots m$ **do**
  Sample a test task $\mathcal{M}_j \sim p(\mathcal{M})$
  $h_{-1} \leftarrow ()$
  for $t = 0 \dots T$ **do**
    $a_t \leftarrow \texttt{DICP}(o_t, h_{t-1}, \theta)$
    $o_{t+1}, r_t \leftarrow$ Perform action a_t on $\mathcal{M}_j$.
    $h_t \leftarrow (h_{t-1}, o_t, a_t, r_t)$
  end for
end for

Algorithm 3 Distillation for In-Context Planning (DICP)

Input: Current observation o_t, learning history h_{t-1}, sequence model θ
Set beam size K, sample size L
$\mathcal{B} \leftarrow \{\}$
for $l = 1 \dots L$ **do**
  $\hat{a}_t \sim f_\theta(\cdot \mid o_t, h_{t-1})$
  $\hat{r}_t, \hat{o}_{t+1}, \hat{R}_t \sim g_\theta(\cdot \mid o_t, \hat{a}_t, h_{t-1})$
  $\hat{h}_t \leftarrow (h_{t-1}, o_t, \hat{a}_t, \hat{r}_t)$
  $\mathcal{B} \leftarrow \mathcal{B} \cup (\hat{h}_t, \hat{o}_{t+1})$
end for
while stopping criterion is not met **do**
  $\mathcal{B}' \leftarrow \{\}$
  for all $(\hat{h}_{s-1}, \hat{o}_s) \in \mathcal{B}$ **do**
    for $l = 1 \dots L$ **do**
      $\hat{a}_s \sim f_\theta(\cdot \mid \hat{o}_s, \hat{h}_{s-1})$
      $\hat{r}_s, \hat{o}_{s+1}, \hat{R}_s \sim g_\theta(\cdot \mid \hat{o}_s, \hat{a}_s, \hat{h}_{s-1})$
      $\hat{h}_s \leftarrow (\hat{h}_{s-1}, \hat{o}_s, \hat{a}_s, \hat{r}_s)$
      $\mathcal{B}' \leftarrow \mathcal{B}' \cup (\hat{h}_s, \hat{o}_{s+1})$
    end for
  end for
  $\mathcal{B} \leftarrow$ Top K elements of $\mathcal{B}'$ w.r.t. $\sum_{t'=t}^{s-1} \hat{r}_{t'} + \hat{R}_s$
end while
$(h_{t-1}, o_t, \hat{a}_t, \hat{r}_t, \dots, \hat{o}_{S+1}) \leftarrow$ Top element of $\mathcal{B}$ w.r.t. $\sum_{t'=t}^{S-1} \hat{r}_{t'} + \hat{R}_S$
Return: $\hat{a}_t$

4 Distillation for In-Context Planning

In this section, we propose *Distillation for In-Context Planning (DICP)*, where the agent utilizes an in-context learned dynamics model to plan actions. To learn the dynamics model in-context, we introduce *meta-model* $g_\theta : \mathcal{H} \times \mathcal{O} \times \mathcal{A} \to \Delta(\mathbb{R}) \times \Delta(\mathcal{O}) \times \Delta(\mathbb{R})$, which shares the same sequence model θ with the algorithm f_θ. It yields probability distributions over the spaces of reward r_t, next observation o_{t+1}, and return-to-go $R_t = \sum_{t'=t}^{H} r_{t'}$ based on history h_{t-1}, current observation o_t, action a_t. H represents the time step at which the episode ends. We optimize θ throughout the meta-training phase (Alg. 1) with following loss:

$$\mathcal{L}(\theta) = \mathcal{L}_{\text{Im}}(\theta) + \lambda \cdot \mathcal{L}_{\text{Dyn}}(\theta), \text{ where } \mathcal{L}_{\text{Dyn}}(\theta) = -\sum_{i=1}^{n} \sum_{t=1}^{T} \log g_\theta(r_t, o_{t+1}, R_t | o_t, a_t, h_{t-1}). \quad (2)$$

Here, $\mathcal{L}_{\text{Im}}$ corresponds to one of $\mathcal{L}_{\text{AD}}$, $\mathcal{L}_{\text{DPT}}$, or $\mathcal{L}_{\text{IDT}}$, and λ is a hyperparameter that balances the imitation loss $\mathcal{L}_{\text{Im}}$ and the dynamics loss $\mathcal{L}_{\text{Dyn}}$.

After meta-training, the sequence model θ is fixed and evaluated during the meta-test phase (Alg. 2). A key distinction between our method and previous in-context RL approaches (Laskin et al., 2023; Lee et al., 2023; Huang et al., 2024) lies in how actions are selected (L6). Previous methods generate actions directly from the sequence model: $a_t \leftarrow f_\theta(\cdot \mid o_t, h_{t-1})$. These approaches may replicate the inefficiencies arising from the gradual updates of gradient-based RL algorithms, as they imitate the source algorithm's behaviors.

In contrast, our method employs an additional `DICP` subroutine (Alg. 3) for action selection. As a planning strategy, we adopt Model Predictive Control (MPC) (Nagabandi et al., 2018; 2019; Sæmundsson et al., 2018). At each time step, the agent simulates future outcomes, selects the path that maximizes predicted return, and executes the first action in that path. Specifically, upon receiving an observation o_t, the agent samples L candidate actions $\{\hat{a}_t^1, \dots, \hat{a}_t^L\}$, and predicts the consequences

of the actions using the dynamics model, which are the next observations $\{\hat{o}_{t+1}^1, \ldots, \hat{o}_{t+1}^L\}$ and rewards $\{\hat{r}_t^1, \ldots, \hat{r}_t^L\}$. The agent also predicts return-to-go $\{\hat{R}_{t+1}^1, \ldots, \hat{R}_t^L\}$ for each candidate action to evaluate each path. The process repeats for future time steps, generating new candidate actions $\{\{\hat{a}_{t+1}^{1,1}, \ldots, \hat{a}_{t+1}^{1,L}\}, \ldots, \{\hat{a}_{t+1}^{L,1}, \ldots, \hat{a}_{t+1}^{L,L}\}\}$ and corresponding consequences, until either the predefined planning horizon is reached or the episode ends. This process constructs a planning tree, where each path is ranked based on the predicted return. The overall DICP algorithm is presented in Alg. 3, where superscripts are omitted for brevity.

After building the planning tree, the agent can apply a suitable tree search algorithm that fits within computational and memory constraints. In our setup, we employ *beam search* as it is well-suited to Transformers, where decoding, sorting, and slicing operations for respective beams are parallelizable. For each planning step, the top K paths are selected based on the predicted return. As demonstrated in §5, when the environment provides well-structured dense rewards, a simple *greedy search* combined with the in-context learned dynamics model achieves competitive performance, although beam search remains applicable in such environments. In Alg. 3, greedy search is represented by skipping the while loop of L10-21.

The DICP algorithm provides a mechanism for the agent to deviate from the source algorithm's suboptimal behaviors and immediately pursue reward-maximizing actions. Since modeling the environment's dynamics is independent of the source algorithm's gradual update rule, the agent can leverage the in-context learned dynamics model to enhance the decision-making process. When the agent identifies promising transitions that contain information for achieving higher returns, the in-context learned dynamics model assigns higher expected returns to prospective state-action pairs that align with this information. When such pairs are sampled (L6 & L14), the dynamics model assigns them higher returns (L7 & L15), encouraging further exploration toward these promising areas (L20 & L22).

Architecture. We assess our framework using architectures from AD (Laskin et al., 2023), DPT (Lee et al., 2023), and IDT (Huang et al., 2024), with modifications to incorporate the additional loss term $\mathcal{L}_{\text{Dyn}}$ as shown in Eq. 2. These modifications are highlighted in Fig. 4 in Appendix. For AD and DPT, the target action a_t is appended to the input sequence, while the reward r_t and next observation o_{t+1} are predicted based on a_t. We also compress each (o, a, r) tuple into a single token, following Lee et al. (2023). For IDT, we have the model predict the rewards and next observations in its Decisions-to-Go module, which directly interacts with the world through low-level actions. However, we observe that the original architecture fails to propagate information about the reward model, as the Reviewing-Decisions module only encodes observations and actions. To resolve this, we modify the Making-Decisions module to also encode rewards. We provide a review of the original contributions of Lee et al. (2023); Huang et al. (2024) in Appendix D.

Distribution choice. For the distribution class of f_θ, we use a categorical distribution for discrete action spaces and a Gaussian distribution with diagonal covariance for continuous ones. For g_θ, we apply the same approach, using a categorical distribution for discrete state spaces and rewards, and a Gaussian for continuous ones. Thus, $\mathcal{L}_{\text{Im}}(\theta)$ and $\mathcal{L}_{\text{Dyn}}(\theta)$ correspond to either cross-entropy loss or Gaussian negative log-likelihood, depending on the environment.

5 Experiments

5.1 Environments

We evaluate our DICP framework across a diverse set of environments. For discrete environments, we use Darkroom, Dark Key-to-Door, and Darkroom-Permuted, which are well-established benchmarks for in-context RL studies (Laskin et al., 2023; Lee et al., 2023; Huang et al., 2024). For continuous ones, we test on the Meta-World benchmark suite (Yu et al., 2019).

Darkroom. Darkroom is a 2D discrete environment where the agent should locate a goal with limited observations. The state space consists of a 9×9 grid, and the action space includes five actions: up, down, left, right, and stay. The agent earns a reward of 1 whenever reaching the goal, with 0 reward otherwise. The agent's observation is restricted to its current position, which makes

it challenging to infer the goal's location. The agent always starts at the center of the grid, and the tasks are distinguished by varying goal locations, resulting in 81 distinct tasks. The tasks are divided into disjoint training and test sets, with a 90:10 split. Each episode has a horizon of 20 steps.

Dark Key-to-Door. Dark Key-to-Door is a variation of Darkroom, where the agent should find a key before reaching the goal. The agent receives a reward of 1 upon finding the key and an additional reward of 1 upon reaching the goal. Unlike Darkroom, the agent only earns a reward from the goal once per episode, with a maximum reward of 2 per episode. This environment features $81 \times 81 = 6561$ distinct tasks, each defined by different key and goal locations. The train-test split ratio is 95:5. The episode horizon is extended to 50 steps.

Darkroom-Permuted. Darkroom-Permuted is another variant of Darkroom, where the action space is randomly permuted. In this environment, the agent starts in a fixed corner of the grid, with the goal located in the opposite corner. There are $5! = 120$ unique tasks, each corresponding to a different permutation of the action space. Since the agent is tested on novel permutations, it must explore the environment to figure out the effects of each action. The train-test split ratio is the same as in Darkroom. The episode horizon is 50 steps.

Meta-World. Meta-World (Yu et al., 2019) is a robotic manipulation benchmark suite designed for meta-RL and multi-task RL. The suite includes 50 continuous control tasks and offers three distinct meta-RL benchmarks: ML1, ML10, and ML45. We focus on ML1, which provides 50 pre-defined seeds for both training and test for each task. Each seed represents a different initialization of the object, goal, and the agent. Although the agent receives dense rewards tailored to each specific task, its performance is evaluated based on the average success rate across test seeds, which differs from the dense reward structure. The episode horizon is 500 steps.

5.2 Baselines

In-context RL methods. We compare our approach with recent in-context model-free methods, including AD (Laskin et al., 2023), DPT (Lee et al., 2023), and IDT (Huang et al., 2024). We follow the evaluation protocols of previous works (Laskin et al., 2023; Huang et al., 2024). For the source algorithms, we use PPO (Schulman et al., 2017) to generate learning histories. We collect data using 100 actors, accumulating a total of 100K to 1M environment steps, depending on the environment. The context length is set to four and ten episode horizons for discrete and continuous environments, respectively. We evaluate DPT only in Darkroom variants because they assume the availability of optimal actions, which are not applicable in general environments.

Other meta-RL methods. For model-free meta-RL methods, we include RL^2 (Duan et al., 2016), MAML (Finn et al., 2017), PEARL (Rakelly et al., 2019), MACAW (Mitchell et al., 2021), and FOCAL (Li et al., 2021). For the model-based methods, we compare against MuZero (Schrittwieser et al., 2019), BOReL (Dorfman et al., 2021), MoSS (Wang et al., 2023b), and IDAQ (Wang et al., 2023a). To ensure a fair comparison, we report IDAQ results using SAC as the source algorithm, rather than expert policies. The original BOReL leverages an oracle reward function, so we report results without it, leading to failure on most tasks as discussed in Dorfman et al. (2021); Wang et al. (2023a). MuZero is not originally designed for meta-RL, but we include it due to its strong performance after pre-training on meta-training tasks followed by fine-tuning on meta-test tasks (Anand et al., 2022). Due to the challenge in reproducing meta-RL approaches, we present the results reported in the original papers, following prior works (Anand et al., 2022; Wang et al., 2023b).

5.3 Results

We begin by comparing our approach with model-free counterparts on the Darkroom, Dark Key-to-Door, and Darkroom-Permuted environments. The first row of Fig. 2 displays the learning curves for these environments. Under our unified configurations and implementations, the best algorithm among AD, DPT, and IDT varies according to environments. Nonetheless, our model-based approach consistently outperforms the model-free counterparts. For planning, we use beam search with a beam size of 10, considering all 5 actions at each planning step. The ablation study over different beam sizes are discussed in §6.1.

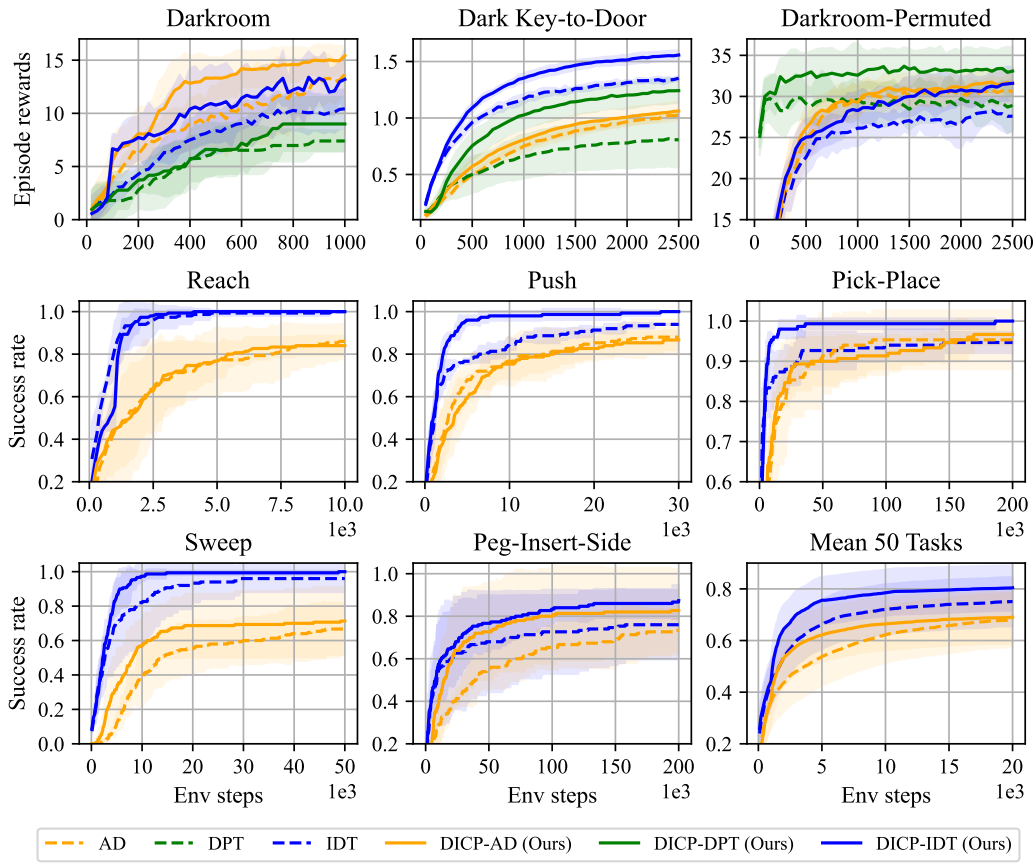

Figure 2: Learning curves of in-context RL approaches during the meta-test phase on discrete (1st row) and continuous (2nd and 3rd rows) environments. Our methods outperform model-free counterparts in both sample efficiency and overall performance. Results are averaged over 5 and 3 train-test splits for discrete and continuous benchmarks, respectively. We also report the mean success rate across all 50 tasks in Meta-World ML1. The final performance results for all ML1 benchmarks are presented in Table 1 and Table 8. Shaded areas represent 95% confidence intervals.

Furthermore, we evaluate our approach on Meta-World ML1 benchmarks against previous meta-RL methods, including both model-free and model-based methods. Table 1 presents the mean success rates over the meta-test phase for *Reach-v2*, *Push-v2*, *Pick-Place-v2*, *Sweep-v2*, and *Peg-Insert-Side-v2*, following previous works (Yu et al., 2019; Anand et al., 2022; Wang et al., 2023b;a). Our method achieves state-of-the-art performance on this benchmarks, surpassing all previous meta-RL methods. A key highlight is that our approach reaches this performance with a maximum of only 200K environment steps, whereas most other methods require at least 10M steps. To ensure a fair comparison with Wang et al. (2023a), whose meta-test is conducted with only 5K environment steps, we also report the results at 5K steps in Table 9. Our approach consistently outperforms the baselines from Wang et al. (2023a) at this step count as well. While in-context model-free baselines (Laskin et al., 2023; Huang et al., 2024) are also relatively sample-efficient, their performance remains suboptimal compared to our method. The learning curves are displayed in the second and third rows of Fig. 2. For planning, we employ greedy search with a sample size of 10 at each step.

6 Ablation Study

We perform an ablation study to evaluate key design choices in our approach. We examine the effect of model-based planning at different scales (§6.1), the effect of context length on the accuracy of the in-context learned dynamics model (§6.2), and the effect of different source algorithms (§6.3).

Table 1: Meta-test success rates on Meta-World ML1. The success rates are reported as percentages, averaged over 3 train-test splits with 50 test seeds. The results marked with * are taken from Yu et al. (2019), while the ones with † are from Wang et al. (2023a). The results for MoSS and MuZero are from Wang et al. (2023b) and Anand et al. (2022), respectively. Our approach achieve state-of-the-art performance with much fewer environment steps. Results at 5K steps are presented in Table 9. We omit '-v2' from the task names.

Method	Reach	Push	Pick-Place	Sweep	Peg-Insert-Side	Max Steps
RL^{2*}	**100**	96	98	–	–	300M
MAML*	**100**	94	80	–	–	300M
PEARL*	68	44	28	–	–	300M
MACAW†	–	–	–	4	0	5K
FOCAL†	–	–	–	38	10	5K
MuZero	**100**	**100**	**100**	–	–	10M
MoSS	86	**100**	**100**	–	–	40M
BoREL†	–	–	–	0	0	5K
IDAQ†	–	–	–	59	30	5K
AD	86	88	96	67	73	200K
IDT	**100**	94	95	96	76	200K
DICP-AD (Ours)	84	87	97	71	83	200K
DICP-IDT (Ours)	**100**	**100**	**100**	**100**	**87**	200K

6.1 Effect of Model-based Planning at Different Scales

We evaluate our approach using search algorithms at varying scales, as shown in the first row of Fig. 3. Experiments are conducted in two environments: Darkroom (discrete) and Reach-v2 (continuous). We use DICP-AD for Darkroom and DICP-IDT for Reach-v2, the best-performing models for each environment. The results demonstrate that incorporating model-based planning significantly improves performance compared to baselines that train the dynamics model but do not use it for planning. While increasing the beam size or sample size improves performance, the gains plateau after a size of 10. When the dynamics model is not used for planning, the performance is comparable to that of model-free baselines.

6.2 Effect of Context Lengths on Accuracy of the Dynamics Model

We investigate the effect of context length on the accuracy of the in-context learned dynamics model. Our hypothesis is that extending the context length enables the model to capture more information about the environment, improving prediction accuracy. To verify this, we evaluate the test loss by forwarding the learning histories of the source algorithm on *meta-test* tasks into the meta-trained DICP-IDT on Reach-v2. The test loss is measured as the mean squared error between the predicted and actual rewards and observations. The models are trained with a context length of 1000, and the loss is calculated by averaging across every 10 positions within the context. The results in the second row of Fig. 3 support our hypothesis: longer context lengths yield more accurate predictions for both observations and rewards. Given that the effectiveness of model-based planning heavily depends on the dynamics model's bias (Janner et al., 2019; Hiraoka et al., 2021), our framework benefits from longer context lengths. Furthermore, as in-context model-free RL methods have also been shown to improve with extended context lengths (Laskin et al., 2023), our combined framework gains substantial advantages from using longer context lengths.

6.3 Effect of Different Source Algorithms

Our framework is agnostic to the choice of the source algorithm, as are previous model-free approaches (Laskin et al., 2023; Lee et al., 2023; Huang et al., 2024). To empirically verify this, we train IDT and DICP-IDT with SAC (Haarnoja et al., 2018) as the source algorithm. As shown in Table 2, our method continues to outperform model-free counterpart. These results demonstrate that our approach is robust to the choice of source algorithm, outperforming model-free baselines

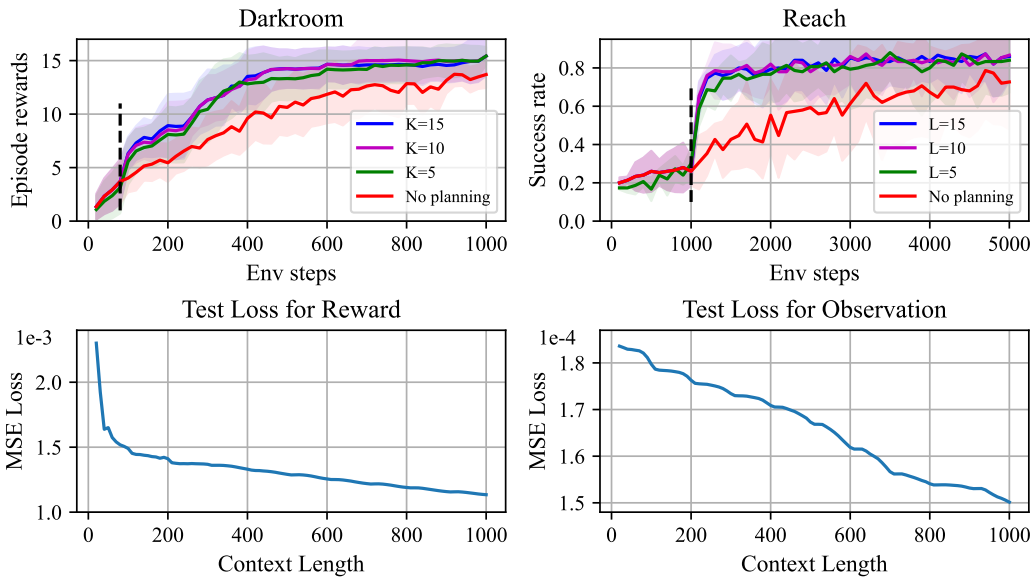

Figure 3: First row: The effect of model-based planning at different scales. We present learning curves with varying beam sizes K and sample sizes L. For the case labeled "No planning," the dynamics model is not utilized for planning, while the meta-model is still trained. The dashed vertical line marks the time step when planning begins, coinciding with the point where the context is fully filled. Second row: The effect of context lengths on the accuracy of the in-context learned dynamics model. Results are averaged over 3 train-test splits.

Table 2: Meta-test success rates of in-context RL approaches using SAC as the source algorithm. Our approach outperforms original model-free IDT. The results are averaged over 3 train-test splits.

Method	Reach	Push	Pick-Place	Sweep	Peg-Insert-Side
IDT	**85**	65	17	**4**	1
DICP-IDT (Ours)	**85**	**69**	**20**	3	**3**

regardless of which source algorithm is used. It is worth noting that since our SAC configuration is not specifically tuned for these tasks, so the overall performance may be underestimated. The hyperparameters for SAC are detailed in Appendix A.

7 Conclusion

We introduced an in-context model-based RL framework that leverages Transformers to not only learn dynamics models but also improve policies in-context. By incorporating model-based planning, our approach effectively addresses the limitations of previous in-context model-free RL methods, which often replicate the suboptimal behavior of the source algorithms. Our framework demonstrated superior performance across various discrete and continuous environments, establishing in-context RL as one of the most effective meta-RL approaches.

A limitation of our approach is the additional computational cost for each action selection compared to model-free methods. However, this trade-off aligns with the current trend of increased computation to fully utilize the reasoning capabilities of Transformers (Brown et al., 2020; Wei et al., 2022). Future work could explore adaptive planning that dynamically adjusts the planning scale based on the context. Incorporating expert demonstrations may also be a meaningful extension that accelerates the learning process. Finally, investigating more advanced or efficient sequence models presents a promising direction for enhancing in-context RL.

Reproducibility Statement

We are committed to ensuring the full reproducibility of our research. The code, included in the supplementary materials, allows for easy replication of all experiments. All datasets used in our experiments can be generated using our code. Detailed configurations are included in both the code and Appendix A. We hope this resource proves valuable to the research community, particularly for newcomers, by offering a unified implementation of in-context RL methods.

References

Ankesh Anand, Jacob C. Walker, Yazhe Li, Eszter Vértes, Julian Schrittwieser, Sherjil Ozair, Theophane Weber, and Jessica B. Hamrick. Procedural generalization by planning with self-supervised world models. In *International Conference on Learning Representations*, 2022.

Tom B. Brown, Benjamin Mann, Nick Ryder, Melanie Subbiah, Jared Kaplan, Prafulla Dhariwal, Arvind Neelakantan, Pranav Shyam, Girish Sastry, Amanda Askell, Sandhini Agarwal, Ariel Herbert-Voss, Gretchen Krueger, Tom Henighan, Rewon Child, Aditya Ramesh, Daniel M. Ziegler, Jeffrey Wu, Clemens Winter, Christopher Hesse, Mark Chen, Eric Sigler, Mateusz Litwin, Scott Gray, Benjamin Chess, Jack Clark, Christopher Berner, Sam McCandlish, Alec Radford, Ilya Sutskever, and Dario Amodei. Language models are few-shot learners. In *Neural Information Processing Systems*, 2020.

Sébastien Bubeck, Varun Chandrasekaran, Ronen Eldan, John A. Gehrke, Eric Horvitz, Ece Kamar, Peter Lee, Yin Tat Lee, Yuan-Fang Li, Scott M. Lundberg, Harsha Nori, Hamid Palangi, Marco Tulio Ribeiro, and Yi Zhang. Sparks of artificial general intelligence: Early experiments with gpt-4. *ArXiv preprint*, 2023.

Lili Chen, Kevin Lu, Aravind Rajeswaran, Kimin Lee, Aditya Grover, Michael Laskin, Pieter Abbeel, Aravind Srinivas, and Igor Mordatch. Decision transformer: Reinforcement learning via sequence modeling. In *Neural Information Processing Systems*, 2021.

Ignasi Clavera, Jonas Rothfuss, John Schulman, Yasuhiro Fujita, Tamim Asfour, and P. Abbeel. Model-based reinforcement learning via meta-policy optimization. In *Conference on Robot Learning*, 2018.

Ron Dorfman, Idan Shenfeld, and Aviv Tamar. Offline meta reinforcement learning - identifiability challenges and effective data collection strategies. In *Neural Information Processing Systems*, 2021.

Alexey Dosovitskiy, Lucas Beyer, Alexander Kolesnikov, Dirk Weissenborn, Xiaohua Zhai, Thomas Unterthiner, Mostafa Dehghani, Matthias Minderer, Georg Heigold, Sylvain Gelly, Jakob Uszkoreit, and Neil Houlsby. An image is worth 16x16 words: Transformers for image recognition at scale. In *International Conference on Learning Representations*, 2021.

Yan Duan, John Schulman, Xi Chen, Peter L. Bartlett, Ilya Sutskever, and P. Abbeel. RL^2: Fast Reinforcement Learning via Slow Reinforcement Learning. *ArXiv preprint*, 2016.

Chelsea Finn, Pieter Abbeel, and Sergey Levine. Model-agnostic meta-learning for fast adaptation of deep networks. In *International Conference on Machine Learning*, 2017.

David Ha and Jürgen Schmidhuber. Recurrent world models facilitate policy evolution. In *Neural Information Processing Systems*, 2018.

Tuomas Haarnoja, Aurick Zhou, Pieter Abbeel, and Sergey Levine. Soft actor-critic: Off-policy maximum entropy deep reinforcement learning with a stochastic actor. In *International Conference on Machine Learning*, 2018.

Danijar Hafner, Jurgis Pasukonis, Jimmy Ba, and Timothy P. Lillicrap. Mastering diverse domains through world models. *ArXiv preprint*, 2023.

Takuya Hiraoka, Takahisa Imagawa, Voot Tangkaratt, Takayuki Osa, Takashi Onishi, and Yoshimasa Tsuruoka. Meta-model-based meta-policy optimization. In *Asian Conference on Machine Learning*, 2021.

Sili Huang, Jifeng Hu, Hechang Chen, Lichao Sun, and Bo Yang. In-context decision transformer: Reinforcement learning via hierarchical chain-of-thought. In *International Conference on Machine Learning*, 2024.

Michael Janner, Justin Fu, Marvin Zhang, and Sergey Levine. When to trust your model: Model-based policy optimization. In *Neural Information Processing Systems*, 2019.

Michael Janner, Qiyang Li, and Sergey Levine. Offline reinforcement learning as one big sequence modeling problem. In *Neural Information Processing Systems*, 2021.

Lukasz Kaiser, Mohammad Babaeizadeh, Piotr Milos, Blazej Osinski, Roy H. Campbell, Konrad Czechowski, Dumitru Erhan, Chelsea Finn, Piotr Kozakowski, Sergey Levine, Afroz Mohiuddin, Ryan Sepassi, George Tucker, and Henryk Michalewski. Model based reinforcement learning for atari. In *International Conference on Learning Representations*, 2020.

Michael Laskin, Luyu Wang, Junhyuk Oh, Emilio Parisotto, Stephen Spencer, Richie Steigerwald, DJ Strouse, Steven Stenberg Hansen, Angelos Filos, Ethan A. Brooks, Maxime Gazeau, Himanshu Sahni, Satinder Singh, and Volodymyr Mnih. In-context reinforcement learning with algorithm distillation. In *International Conference on Learning Representations*, 2023.

Jonathan Lee, Annie Xie, Aldo Pacchiano, Yash Chandak, Chelsea Finn, Ofir Nachum, and Emma Brunskill. Supervised pretraining can learn in-context reinforcement learning. In *Neural Information Processing Systems*, 2023.

Kuang-Huei Lee, Ofir Nachum, Mengjiao Yang, L. Y. Lee, Daniel Freeman, Winnie Xu, Sergio Guadarrama, Ian S. Fischer, Eric Jang, Henryk Michalewski, and Igor Mordatch. Multi-game decision transformers. In *Neural Information Processing Systems*, 2022.

Sergey Levine, Aviral Kumar, G. Tucker, and Justin Fu. Offline reinforcement learning: Tutorial, review, and perspectives on open problems. *ArXiv preprint*, 2020.

Lanqing Li, Rui Yang, and Dijun Luo. FOCAL: efficient fully-offline meta-reinforcement learning via distance metric learning and behavior regularization. In *International Conference on Learning Representations*, 2021.

Zichuan Lin, Garrett Thomas, Guangwen Yang, and Tengyu Ma. Model-based adversarial meta-reinforcement learning. In *Neural Information Processing Systems*, 2020.

Hao Liu and P. Abbeel. Emergent agentic transformer from chain of hindsight experience. In *International Conference on Machine Learning*, 2023.

Eric Mitchell, Rafael Rafailov, Xue Bin Peng, Sergey Levine, and Chelsea Finn. Offline meta-reinforcement learning with advantage weighting. In *International Conference on Machine Learning*, 2021.

Anusha Nagabandi, Gregory Kahn, Ronald S. Fearing, and Sergey Levine. Neural network dynamics for model-based deep reinforcement learning with model-free fine-tuning. *IEEE International Conference on Robotics and Automation*, 2018.

Anusha Nagabandi, Ignasi Clavera, Simin Liu, Ronald S. Fearing, Pieter Abbeel, Sergey Levine, and Chelsea Finn. Learning to adapt in dynamic, real-world environments through meta-reinforcement learning. In *International Conference on Learning Representations*, 2019.

Alex Nichol, Joshua Achiam, and John Schulman. On first-order meta-learning algorithms. *ArXiv preprint*, 2018.

Brieuc Pinon, Jean-Charles Delvenne, and Raphaël M. Jungers. A model-based approach to meta-reinforcement learning: Transformers and tree search. *European Symposium on Artificial Neural Networks, Computational Intelligence and Machine Learning*, 2022.

Antonin Raffin, Ashley Hill, Adam Gleave, Anssi Kanervisto, Maximilian Ernestus, and Noah Dormann. Stable-baselines3: Reliable reinforcement learning implementations. *Journal of Machine Learning Research*, 2021.

Kate Rakelly, Aurick Zhou, Chelsea Finn, Sergey Levine, and Deirdre Quillen. Efficient off-policy meta-reinforcement learning via probabilistic context variables. In *International Conference on Machine Learning*, 2019.

Scott Reed, Konrad Zolna, Emilio Parisotto, Sergio Gomez Colmenarejo, Alexander Novikov, Gabriel Barth-Maron, Mai Gimenez, Yury Sulsky, Jackie Kay, Jost Tobias Springenberg, Tom Eccles, Jake Bruce, Ali Razavi, Ashley D. Edwards, Nicolas Manfred Otto Heess, Yutian Chen, Raia Hadsell, Oriol Vinyals, Mahyar Bordbar, and Nando de Freitas. A generalist agent. *Transactions on Machine Learning Research*, 2022.

Zohar Rimon, Aviv Tamar, and Gilad Adler. Meta reinforcement learning with finite training tasks - a density estimation approach. In *Neural Information Processing Systems*, 2022.

Zohar Rimon, Tom Jurgenson, Orr Krupnik, Gilad Adler, and Aviv Tamar. Mamba: an effective world model approach for meta-reinforcement learning. In *International Conference on Learning Representations*, 2024.

Steindór Sæmundsson, Katja Hofmann, and Marc Peter Deisenroth. Meta reinforcement learning with latent variable gaussian processes. In *Conference on Uncertainty in Artificial*, 2018.

Julian Schrittwieser, Ioannis Antonoglou, Thomas Hubert, Karen Simonyan, L. Sifre, Simon Schmitt, Arthur Guez, Edward Lockhart, Demis Hassabis, Thore Graepel, Timothy P. Lillicrap, and David Silver. Mastering atari, go, chess and shogi by planning with a learned model. *Nature*, 2019.

Julian Schrittwieser, Thomas Hubert, Amol Mandhane, Mohammadamin Barekatain, Ioannis Antonoglou, and David Silver. Online and offline reinforcement learning by planning with a learned model. In *Neural Information Processing Systems*, 2021.

John Schulman, Sergey Levine, Pieter Abbeel, Michael I. Jordan, and Philipp Moritz. Trust region policy optimization. In *International Conference on Machine Learning*, 2015.

John Schulman, Filip Wolski, Prafulla Dhariwal, Alec Radford, and Oleg Klimov. Proximal policy optimization algorithms. *ArXiv preprint*, 2017.

Viacheslav Sinii, Alexander Nikulin, Vladislav Kurenkov, Ilya Zisman, and Sergey Kolesnikov. In-context reinforcement learning for variable action spaces. In *International Conference on Machine Learning*, 2024.

Ashish Vaswani, Noam Shazeer, Niki Parmar, Jakob Uszkoreit, Llion Jones, Aidan N. Gomez, Lukasz Kaiser, and Illia Polosukhin. Attention is all you need. In *Neural Information Processing Systems*, 2017.

Jane X. Wang, Zeb Kurth-Nelson, Hubert Soyer, Joel Z. Leibo, Dhruva Tirumala, Rémi Munos, Charles Blundell, Dharshan Kumaran, and Matthew M. Botvinick. Learning to reinforcement learn. *ArXiv preprint*, 2016.

Jianhao Wang, Jin Zhang, Haozhe Jiang, Junyu Zhang, Liwei Wang, and Chongjie Zhang. Offline meta reinforcement learning with in-distribution online adaptation. In *International Conference on Machine Learning*, 2023a.

Mingyang Wang, Zhenshan Bing, Xiangtong Yao, Shuai Wang, Hang Su, Chenguang Yang, Kai Huang, and Alois Knoll. Meta-reinforcement learning based on self-supervised task representation learning. In *AAAI Conference on Artificial Intelligence*, 2023b.

Jason Wei, Xuezhi Wang, Dale Schuurmans, Maarten Bosma, Ed Huai hsin Chi, F. Xia, Quoc Le, and Denny Zhou. Chain of thought prompting elicits reasoning in large language models. In *Neural Information Processing Systems*, 2022.

Weirui Ye, Shaohuai Liu, Thanard Kurutach, Pieter Abbeel, and Yang Gao. Mastering atari games with limited data. In *Neural Information Processing Systems*, 2021.

Tianhe Yu, Deirdre Quillen, Zhanpeng He, Ryan C. Julian, Karol Hausman, Chelsea Finn, and Sergey Levine. Meta-world: A benchmark and evaluation for multi-task and meta reinforcement learning. In *Conference on Robot Learning*, 2019.

Haoqi Yuan and Zongqing Lu. Robust task representations for offline meta-reinforcement learning via contrastive learning. In *International Conference on Machine Learning*, 2022.

Peiyuan Zhang, Guangtao Zeng, Tianduo Wang, and Wei Lu. Tinyllama: An open-source small language model. *ArXiv preprint*, 2024.

Luisa M. Zintgraf, Kyriacos Shiarlis, Maximilian Igl, Sebastian Schulze, Yarin Gal, Katja Hofmann, and Shimon Whiteson. Varibad: A very good method for bayes-adaptive deep RL via meta-learning. In *International Conference on Learning Representations*, 2020.

Luisa M. Zintgraf, Leo Feng, Cong Lu, Maximilian Igl, Kristian Hartikainen, Katja Hofmann, and Shimon Whiteson. Exploration in approximate hyper-state space for meta reinforcement learning. In *International Conference on Machine Learning*, 2021.

Ilya Zisman, Vladislav Kurenkov, Alexander Nikulin, Viacheslav Sinii, and Sergey Kolesnikov. Emergence of in-context reinforcement learning from noise distillation. In *International Conference on Machine Learning*, 2024.

A Implementation Details

A.1 Source Algorithms

For the source algorithms (Schulman et al., 2017; Haarnoja et al., 2018), we use the implementation of Stable Baselines 3 (Raffin et al., 2021). The hyperparamter settings are detailed in Table 3-4. Unless otherwise specified, most hyperparameters are set to default values.

Table 3: Hyperparamters for the source PPO algorithm.

Hyperparmater	Darkroom	Dark Key-to-Door	Darkroom-Permuted	Meta-World
learning_rate	3e-4	3e-4	3e-4	3e-4
n_steps	20	50	50	100
batch_size	50	100	50	200
n_epochs	20	10	20	20
γ	0.99	0.99	0.99	0.99
total_timesteps	100K	100K	100K	1M

Table 4: Hyperparamters for the source SAC algorithm.

Hyperparmater	Meta-World
learning_rate	3e-4
learning_starts	100
batch_size	128
train_freq	10
gradient_steps	1
buffer_size	1M
γ	0.99
total_timesteps	1M

A.2 Transformers

We implement Transformers using the open-source TinyLlama (Zhang et al., 2024). The hyperparameters are provided in Table 5, along with additional parameters specific to IDT.

Table 5: Hyperparamters for Transformers. All three Transformer modules in IDT share the same set of hyperparameters.

Hyperparmater	AD/DPT (disc.)	IDT (disc.)	AD (cont.)	IDT (cont.)
n_layer	4	4	4	4
n_head	4	4	8	4
n_embed	32	32	64	32
intermediate_size	128	128	256	128
dropout	0.1	0.1	0.1	0.1
attention_dropout	0.1	0.1	0.1	0.1
optimizer	AdamW	AdamW	AdamW	AdamW
scheduler	cosine decay	cosine decay	cosine decay	cosine decay
learning_rate (at start)	1e-2	1e-3	1e-2	1e-3
β_1	0.9	0.9	0.9	0.9
β_2	0.99	0.99	0.99	0.99
weight_decay	0.01	0.01	0.01	0.01
λ	1	1	1	1
n_actions per high-level decision	–	10	–	10
dim_z	–	8	–	8

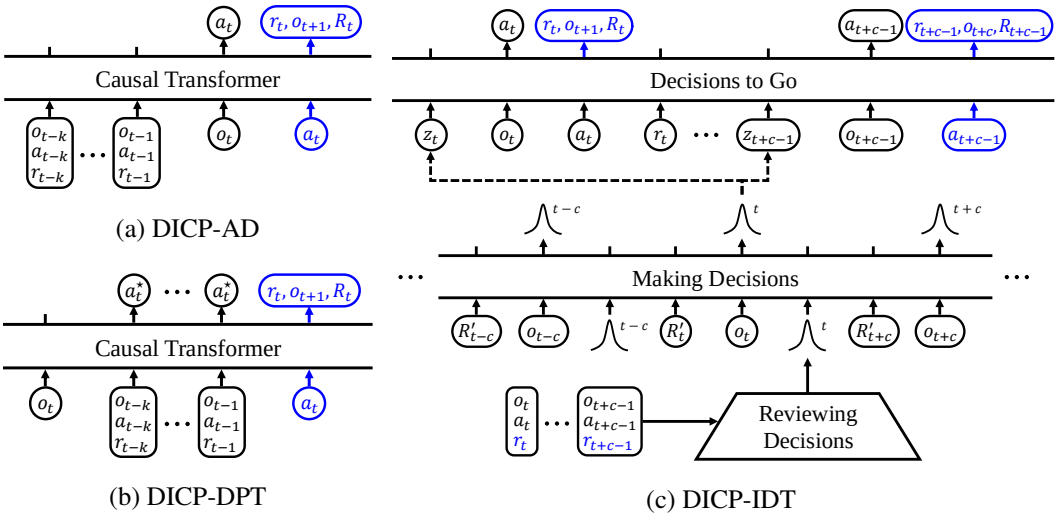

Figure 4: Model-based adaptation of in-context RL methods for DICP. The notations are defined as follows: z: high-level decisions, R: return-to-go, k: the number of transitions within the context, c: the number of low-level actions guided by a single high-level decision, and R': relabeled return-to-go, following (Huang et al., 2024). Newly introduced components are highlighted in blue.

Table 6: Hyperparamters for planning.

Hyperparmater	Darkroom	Dark Key-to-Door	Darkroom-Permuted	Meta-World
planning horizon	8	16	16	1
beam size (K)	10	10	10	–
sample size (L)	5	5	5	10

A.3 Environments

In the ML1 benchmarks, we observe that using shorter horizons for the source algorithm accelerates the learning of in-context RL methods. Specifically, we terminate the source algorithm after 100 steps, as opposed to the original 500-step horizon provided by Meta-World. To minimize train-test discrepancies, we also meta-test the in-context RL methods using 100-step horizons. Even under these less favorable conditions, in-context RL methods still outperform the baselines, as shown in Fig. 2 and Table 1.

A.4 Planning

We find that predicting only the immediate reward, rather than both the immediate reward and the return-to-go, is sufficient to outperform baselines. Summation of predicted immediate rewards up to the current step can serve as a myopic proxy for the total return of a planning path. In Dark-room variants, the binary nature of rewards often leads to different beam paths achieving the same

Table 7: FLOPs per action selection.

Method	Darkroom	Dark Key-to-Door	Darkroom-Permuted	Meta-World
AD	6M	20M	20M	709M
DPT	6M	20M	20M	709M
IDT	8M	8M	8M	3M
DICP-AD	2G	18G	18G	8G
DICP-DPT	2G	18G	18G	8G
DICP-IDT	147M	147M	147M	15M

cumulative reward during planning. When such ties arise, we break them by following the model's preference during action generation. This approach allows the agent to behave like a model-free counterpart when the goal or key is distant, while benefiting from model-based planning when the dynamics model can confidently predict rewards over shorter horizons. In Meta-World, the dense, human-designed reward structure further improves the effectiveness of this myopic return estimation. Since the rewards are designed to guide the agent toward the goal by greedily following reward increases, ranking planning paths based on immediate rewards often sufficient to improve in-context RL approaches. Hyperparamters for planning are detailed in Table 6.

Table 8: Results on all benchmarks of Meta-World ML1. We omit the rows for the 5 tasks reported in Table 1, while they are still included in the mean calculation.

Task	AD	IDT	DICP-AD (Ours)	DICP-IDT (Ours)
Assembly	0	2	**28**	4
Basketball	50	54	48	**66**
Bin-Picking	2	**6**	0	**6**
Box-Close	34	32	**44**	38
Button-Press-Topdown	98	**100**	**100**	**100**
Button-Press-Topdown-Wall	98	**100**	**100**	**100**
Button-Press	**100**	**100**	**100**	**100**
Button-Press-Wall	**100**	**100**	**100**	**100**
Coffee-Button	**100**	**100**	**100**	**100**
Coffee-Pull	88	78	42	**90**
Coffee-Push	98	**100**	92	**100**
Dial-Turn	76	76	30	**94**
Disassemble	0	0	0	0
Door-Close	**100**	**100**	**100**	**100**
Door-Lock	98	**100**	88	98
Door-Open	78	14	**90**	80
Door-Unlock	78	72	74	**82**
Hand-Insert	84	70	**86**	68
Drawer-Close	**100**	**100**	**100**	**100**
Drawer-Open	26	46	62	**90**
Faucet-Open	**100**	**100**	96	98
Faucet-Close	**100**	**100**	86	**100**
Hammer	8	22	**52**	10
Handle-Press-Side	**100**	**100**	94	**100**
Handle-Press	**100**	**100**	**100**	**100**
Handle-Pull-Side	36	**100**	82	**100**
Handle-Pull	56	66	74	**78**
Lever-Pull	96	96	**100**	98
Pick-Place-Wall	6	66	6	**70**
Pick-Out-Of-Hole	36	**98**	2	86
Plate-Slide	92	**96**	94	90
Plate-Slide-Side	**100**	**100**	**100**	**100**
Plate-Slide-Back	92	**98**	88	86
Plate-Slide-Back-Side	94	**100**	**100**	96
Peg-Unplug-Side	86	**100**	38	98
Soccer	94	96	92	**100**
Stick-Push	**2**	0	0	**2**
Stick-Pull	2	14	0	**50**
Push-Wall	86	94	92	**100**
Push-Back	0	0	0	0
Reach-Wall	**100**	98	94	**100**
Shelf-Place	0	**68**	0	62
Sweep-Into	86	86	**88**	**88**
Window-Open	**100**	**100**	**100**	**100**
Window-Close	**100**	**100**	88	98
Mean	68	75	69	**80**

While model-based planning requires additional computation, the cost is negligible. Specifically, our method does not increase the number of training parameters compared to model-free counter-

parts, and the primary difference lies in the increased number of Transformer inferences per action selection. As shown in Table 7, the maximum computation per action selection is approximately 18 GFLOPs in our experiment. Given that modern GPUs can process hundreds of teraFLOPs per second, the computational expense is minimal in practice while the performance gains are substantial, making the trade-off highly favorable in our framework. The difference becomes even less significant when using architectures like IDT, which are specifically designed to handle longer sequences efficiently.

B Additional Experiments

We conducted experiments across all 50 environments of Meta-World ML1, using PPO (Schulman et al., 2017) as the source algorithm with the same hyperparameters as those used in Table 1. Each method is evaluated with 20K environment steps during the meta-test phase. As shown in Table 8, our method outperforms model-free counterparts. The mean learning curve is displayed in Fig. 2. It is noteworthy that since our configuration for the source algorithm is not tuned for every task, the results may not fully reflect the full potential of in-context RL methods, including ours.

Table 9: Meta-test success rates with 5K environment steps on 5 benchmarks of ML1. The results marked with † are taken from Wang et al. (2023a). Our approach consistently outperforms all the baselines at 5K steps as well.

Method	Sweep	Peg-Insert-Side	Steps
MACAW†	4	0	5K
FOCAL†	38	10	5K
BoREL†	0	0	5K
IDAQ†	59	30	5K
IDT	71	41	5K
DICP-IDT (Ours)	**87**	**45**	5K

Furthermore, we also conducted experiments on ML10 from Meta-World, a benchmark designed to evaluate the generalization ability of meta-RL methods using ten predefined training tasks and five test tasks. The results, presented in Table 10, demonstrate that our approach surpasses the model-free counterpart and achieves state-of-the-art performance on this benchmark with significantly fewer environment steps than the baselines. Notably, our method does not rely on expert demonstrations or task descriptions for the test tasks.

Table 10: Meta-test success rates on Meta-World ML10. The success rates are reported as percentages, averaged over 3 different seeds. The results marked with * are taken from Yu et al. (2019).

Method	Success Rate	Steps
PEARL*	13.0	350M
MAML*	31.6	350M
RL^{2}*	35.8	350M
IDT	36.7	500K
DICP-IDT (Ours)	**46.9**	500K

C Additional Ablation Study

Table 11 shows the direct relationship between world model accuracy and final performance. As the accuracy evolves over time steps in our framework, making it difficult to establish the direct relationship between accuracy and performance, we conducted an additional ablation study using a **scripted** world model. This model generates perfect predictions with probability $1 - \epsilon$ and random predictions with probability ϵ. Importantly, our approach is lower-bounded with the "Without Plan-

ning" case by avoiding relying on the world model when it becomes unreliable, ensuring inherent robustness.

Table 11: Episode rewards after 50 test episodes of DICP-AD in Darkroom with different ϵ of scripted world model. The results are averaged over 5 train-test splits.

ϵ of scripted world model	Episode Rewards
0.00	15.925
0.05	12.175
0.10	8.350
0.15	6.825
0.20	6.825
0.25	6.225
0.30	4.825
Without Planning	14.825

D Extended Related Work

DPT. Decision-Pretrained Transformer (DPT; Lee et al. (2023)) is an in-context RL approach that meta-trains (or pre-trains) Transformers to predict *optimal* actions based on contextual trajectories. Consequently, DPT requires access to the optimal actions during training. The authors suggest several sources for gathering the meta-training dataset, including (i) randomly sampled trajectories directly from the environment, (ii) trajectories generated by a source RL algorithm, and (iii) trajectories of an expert policy. In this work, we concentrate on the second source to minimize reliance on direct access to environment dynamics and expert policies. While the authors also discuss deploying DPT when offline datasets of the *meta-test* tasks are available, our focus is on scenarios where only offline datasets for *meta-train* tasks are available for a fair comparison. In this scheme, the loss function of DPT is defined as

$$\mathcal{L}_{\text{DPT}}(\theta) = -\sum_{i=1}^{n}\sum_{t=1}^{T} \log f_\theta(a_t^\star \mid o_t^i, h_{t-1}^i), \tag{3}$$

where $a_t^\star$ denotes the optimal action on the true state s_t.

IDT. In-Context Decision Transformer (IDT; Huang et al. (2024)) addresses the high computational costs of previous in-context RL methods, particularly when handling long-horizon tasks. IDT restructures the decision-making process to predict high-level decisions instead of individual actions. These high-level decisions then guide multiple action steps in a separate module, dividing the Transformer used in the earlier approach (Laskin et al., 2023) into modules with shorter sequences. The architecture of IDT consists of three modules: (i) the Making-Decisions module predicts high-level decisions, (ii) the Decisions-to-Go module decodes these high-level decisions into low-level actions, and (iii) the Reviewing-Decisions module encodes the resulting low-level actions back into high-level decisions. The loss function for IDT is structured similarly to that of AD, while the loss can be divided across the three modules:

$$\begin{aligned}\mathcal{L}_{\text{IDT}}(\theta) &= -\sum_{i=1}^{n}\sum_{t=1}^{T} \log f_\theta(a_t^i \mid o_t^i, h_{t-1}^i) \\ &= -\sum_{i=1}^{n}\sum_{t=1}^{T} \left[\log f_\theta(a_t^i \mid z_t, o_t^i) + \log f_\theta(z_t \mid o_t^i, \hat{z}_{t-1}) + \log f_\theta(\hat{z}_{t-1} \mid h_{t-1}^i)\right],\end{aligned} \tag{4}$$

where z_t is a high-level decision and $\hat{z}_{t-1}$ is an encoded context by the Reviewing-Decisions module.

TTO. TTO (Janner et al., 2021) is an offline RL approach that imitates the policy of the offline dataset, while simultaneously learning a dynamics model to facilitate planning to improve upon that policy. Our approach is similar to this in that we also use model-based planning to improve upon

offline datasets. However, our framework focuses on improving a distilled algorithm rather than a specific policy. This distinction makes our problem setting more general and challenging compared to single-task RL like TTO, since our agent should learn the dynamics model primarily in-context when encountering novel tasks.

Model-based RL. Model-based RL has gained significant attention due to its ability to improve sample efficiency by utilizing a dynamics model to generate simulated experiences (Ha & Schmidhuber, 2018; Kaiser et al., 2020; Janner et al., 2019; Schrittwieser et al., 2019; Ye et al., 2021; Hafner et al., 2023). Some approaches further incorporate planning with search algorithms, such as MCTS (Schrittwieser et al., 2019; 2021; Ye et al., 2021) or beam search (Janner et al., 2021), to explore the planning space effectively. However, a key challenge in model-based RL is managing the balance between sample efficiency and model bias, as errors in the learned dynamics model can lead to suboptimal decision-making (Janner et al., 2019).

Model-based Meta-RL. Previous approaches have explored model-based approach to meta-RL (Sæmundsson et al., 2018; Lin et al., 2020; Hiraoka et al., 2021; Rimon et al., 2022). Clavera et al. (2018) aim to overcome the limitations of model-based RL (Janner et al., 2019) by incorporating a meta-model. Nagabandi et al. (2019) improve upon model-free meta-RL methods (Duan et al., 2016; Finn et al., 2017) to adapt shifting dynamics. Anand et al. (2022) focus on zero-shot generalization, adapting MuZero (Schrittwieser et al., 2019) to meta-RL. More recently, Rimon et al. (2024) introduce a model-based meta-RL approach that combines a meta-RL method (Zintgraf et al., 2020) with a model-based RL method (Hafner et al., 2023).